

## Structure and Properties of van der Waals Molecules

George E. Ewing

*Department of Chemistry, Indiana University, Bloomington, Indiana 47401*

*Received October 1, 1974*

Gaseous argon cooled to its boiling point contains a few percent of the dimer  $\text{Ar}_2$ . Similarly, cooled nitrogen, oxygen, or hydrogen contains low concentrations of  $(\text{N}_2)_2$ ,  $(\text{O}_2)_2$ , or  $(\text{H}_2)_2$  in the gas phase.

These weakly bound complexes held together by intermolecular forces are called van der Waals molecules. Since intermolecular forces are associated with all atoms and molecules, we should expect the presence of van der Waals molecules, at least in trace amounts, in any gas. In the past several years, refined experimental techniques have allowed the structure and properties of a dozen or so van der Waals molecules to be described. Aside from the curiosity aroused by a new class of compounds, the study of van der Waals molecules is beginning to provide a detailed mapping of intermolecular potential surfaces.

Spectroscopic techniques are particularly promising for the study of van der Waals molecules. Their structure and properties have been revealed by uv, ir, microwave, radiofrequency, and Raman spectroscopy. The emphasis in this Account is on what some of the recent results of these studies have told us about van der Waals molecules; this complements an earlier review of the subject.<sup>1</sup>

### Diatomic van der Waals Molecules

The rare gases Ne, Ar, Kr, and Xe absorb light in the vacuum ultraviolet to give characteristic atomic line spectra. However, under appropriate conditions of pressure and temperature, a multitude of weak additional features are observed. It is the vibrational and rotational levels of  $\text{Ne}_2$ ,  $\text{Ar}_2$ ,  $\text{Kr}_2$ , or  $\text{Xe}_2$  which are involved in the electronic transitions that account for these new weak features.

As an example, the bottom of Figure 1 shows a portion of the absorption of gaseous argon at 10 Torr and 77 K from the work of Tanaka and Yoshino.<sup>2</sup> The intense absorption near 1067 Å is assigned to the transition of atomic argon,  $^3\text{P}_1^0 \leftarrow ^1\text{S}_0$ , indicating the promotion of an electron from the filled  $3p^6(^1\text{S}_0)$  state to form the  $3p^54s(^3\text{P}_1^0)$  state. The fine

structure to longer wavelengths is due to absorption by the  $\text{Ar}_2$  van der Waals molecule.

This molecule consists of two weakly bound  $^1\text{S}_0$  argon atoms and is represented by  $\text{Ar}_2(^1\Sigma_g^+)$ . The upper state is the complex of  $^1\text{S}_0$  with a  $^3\text{P}_1^0$  atom and is labeled  $\text{Ar}_2^*(^1\Sigma_u^+)$ . Assignments of vibrational transitions from the  $v$  levels of the van der Waals molecule to the  $v'$  vibrational levels of the  $^1\Sigma_u^+$  are identified in the spectrum. Transitions between a few of these levels are shown in the upper part of the figure. Finer structure features in the spectrum are due to rotational transitions which are not now assigned.

The dissociation energy of diatomic van der Waals molecules and the width of the potential well can be inferred from the spacings of the vibrational levels. In Figure 1 a Morse potential for  $\text{Ar}_2$  has been fit to the spectroscopic data. The dissociation energy is  $D_0 = 0.92$  kJ/mol ( $76.9$   $\text{cm}^{-1}$ ), or hundreds of times smaller than that of a typical chemically bonded molecule (e.g., for  $\text{H}_2$ ,  $D_0 = 432$  kJ/mol).<sup>3</sup>

Atomic beam scattering data and spectroscopy work well together to give an accurate description of the intermolecular potential function. The results of the elegant scattering experiments of Parson, Siska, and Lee<sup>4</sup> together with the spectroscopic measurements have been described by an eight-parameter intermolecular potential function. This function consists of a Morse potential together with van der Waals attractive terms such as  $R^{-6}$  and  $R^{-8}$  smoothly joined by polynomial terms in the intermolecular distance  $R$ . The resulting Morse-Spline-van der Waals or MSV function for  $\text{Ar}_2$  is shown in Figure 2.

Dissociation energies of rare gas van der Waals molecules range from about 0.2 kJ/mol for  $\text{Ne}_2$ <sup>5</sup> to 2.2 kJ/mol for  $\text{Xe}_2$ .<sup>6</sup> Intermolecular forces are apparently too weak to allow the formation of bound states of the  $\text{He}_2$  van der Waals molecule.<sup>7</sup> The dissociation energies and potential functions from spectroscopic and scattering data for rare gas dimers are

- (1) G. E. Ewing, *Angew. Chem., Int. Ed. Engl.*, 11, 486 (1972).
- (2) Y. Tanaka and K. Yoshino, *J. Chem. Phys.*, 53, 2012 (1970).
- (3) G. Herzberg, "Spectra of Diatomic Molecules", Van Nostrand, Princeton, N.J., 1950.
- (4) J. M. Parson, P. F. Siska, and Y. T. Lee, *J. Chem. Phys.*, 56, 1511 (1972).
- (5) Y. Tanaka and K. Yoshino, *J. Chem. Phys.*, 57, 2964 (1972).
- (6) K. Docken and T. P. Schafer, *J. Mol. Spectrosc.*, 46, 454 (1973).
- (7) Y. Tanaka and K. Yoshino, *J. Chem. Phys.*, 50, 3087 (1969).

George Ewing was an undergraduate at Yale University. He first really learned chemistry from George Pimentel at the University of California (Berkeley) and obtained his Ph.D. degree in 1960. After 3 years as a staff scientist at the Jet Propulsion Laboratory in Pasadena, Calif., he came to Indiana University and is now Professor of Chemistry. Besides his work on van der Waals molecules he is interested in energy transfer in liquids, biophysical chemistry, and writing children's stories.

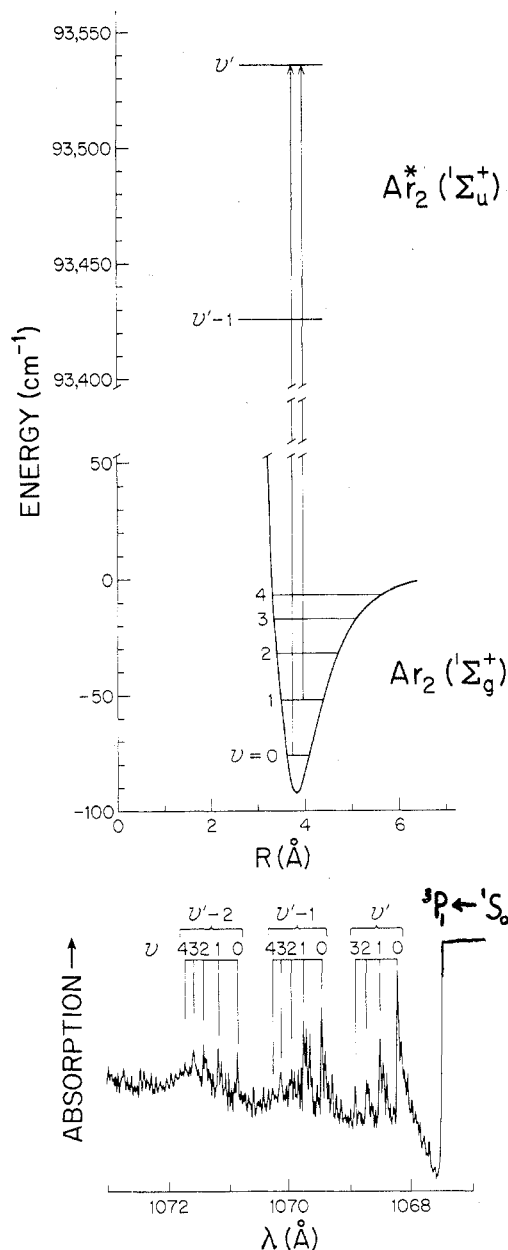


**Figure 1.** Electronic absorption spectrum of Ar<sub>2</sub>. A portion of the absorption spectrum of 10 Torr of argon at 77 K from a densitometer trace of the photographic plate [Y. Tanaka, private communication]. The potential curve of Ar<sub>2</sub> (<sup>1</sup>Σ<sub>g</sub><sup>+</sup>) is derived from the spectroscopic data [Y. Tanaka and K. Yoshino, *J. Chem. Phys.*, 53, 2012 (1970)]. For the <sup>1</sup>Σ<sub>u</sub><sup>+</sup> state neither the absolute vibrational quantum numbers nor the shape of the potential are known. Examples of two electronic-vibrational transitions are shown.

in essential agreement with recent refined treatments of macroscopic properties of the gaseous and condensed phases.<sup>8</sup> All these results point out the approximate nature of the simple Morse or Lennard-Jones 6-12 potentials.

The total number of bound states of van der Waals molecules includes both vibrational and rotational levels, and these must be considered in discussing their properties. The effective potential,  $V_{\text{eff}}$ , between two atoms depends on the potential energy of interaction,  $V(R)$  (e.g., Lennard-Jones 6-12, MSV etc.), and the centrifugal potential which tends to

(8) See, for example, (a) J. A. Barker, R. A. Fisher, and R. D. Watts, *Mol. Phys.*, 21, 657 (1971), or (b) J. A. Barker in "Rare Gas Solids", M. L. Klein and J. A. Venables, Ed., Academic Press, New York, N.Y., 1975, Chapter 4.

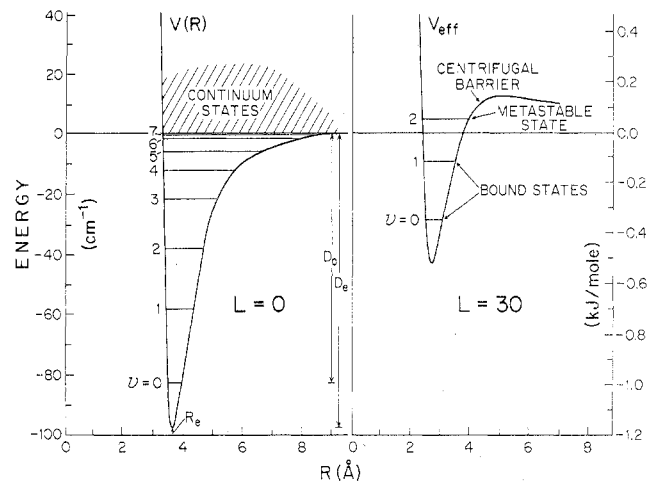


**Figure 2.** Intermolecular potential for Ar<sub>2</sub>. On the left is the MSV III potential curve as given by Parson, Siska, and Lee<sup>4</sup> for nonrotating ( $L = 0$ ) Ar<sub>2</sub>. On the right the effective potential for rotating Ar<sub>2</sub> ( $L = 30$ ). The vibration-rotation energy levels are from calculations of Docken and Schafer.<sup>6</sup>

pull them apart as they rotate (eq 1). The angular

$$V_{\text{eff}} = V(R) + \frac{\hbar^2 L(L+1)}{2\mu R^2} \quad (1)$$

momentum of the pair, of reduced mass  $\mu$ , is indicated by the quantum number  $L$ .

In Figure 2 is a comparison of the potentials for the nonrotating ( $L = 0$ ) and a rotating (e.g.,  $L = 30$ ) Ar<sub>2</sub> van der Waals molecule. For  $L = 0$  there are eight vibrational levels, as shown in Figure 2. The continuum of argon energies above the dissociation limit corresponds to colliding pairs of atoms or continuum states and does not represent van der Waals molecules. For  $L = 30$  the effective potential has a more shallow well, and only two vibrational states reside below the dissociation limit. The energy levels shown were calculated from the MSV potential.<sup>6</sup> The total number of bound  $v$  and  $L$  states for Ar<sub>2</sub> is about 170.<sup>9</sup> Other estimates on diatomic van der Waals molecules range from several bound states for HeNe<sup>5</sup> to over 200,000 for CsXe.<sup>10</sup>

Another property of van der Waals molecules can be seen by examining Figure 2. Rotating molecules with energies above the dissociation limit but beneath the centrifugal barrier reside in metastable states. In principle these molecules can "tunnel" or "leak through" this barrier. The lifetimes estimated for different states of Ar<sub>2</sub> range from  $10^{-11}$  sec near the top of the barrier to  $10^{10}$  sec for a metastable state well below the barrier.<sup>11</sup> This enormous range in lifetimes is also found in calculations for other van der Waals molecules.<sup>12</sup>

The lifetime of van der Waals molecules is usually limited not by tunnelling but by the time between collisions. This is because the dissociation energy is so small that almost every gas-phase collision will be effective in dissociating the van der Waals molecule. At a pressure of 1 atm and 300 K this time is of the order of  $10^{-10}$  sec, and at 1 Torr it becomes of the order of  $10^{-7}$  sec.<sup>13</sup> Optical pumping experiments on

(9) J. K. Cashion, *J. Chem. Phys.*, 48, 94 (1968).

(10) G. D. Mahan, *J. Chem. Phys.*, 52, 258 (1970).

(11) D. E. Stogryn and J. O. Hirschfelder, *J. Chem. Phys.*, 31, 1531 (1959).

(12) W. E. Baylis, *Phys. Rev. A*, 1, 990 (1970).

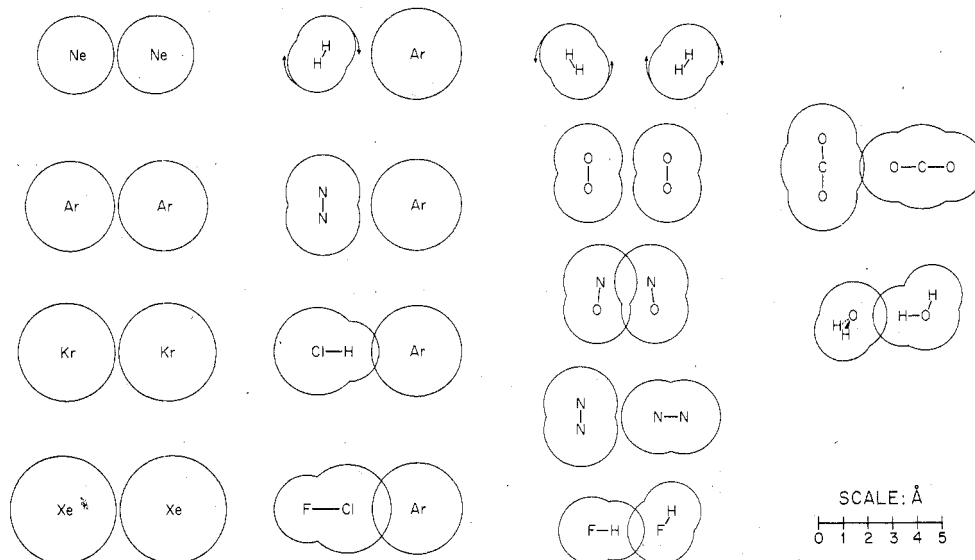


Figure 3. The structure of some van der Waals molecules. The spheres around each atom have radii equal to their van der Waals radii. The structural parameters are discussed in the text.

alkali metal-rare gas van der Waals molecules (e.g.,  $\text{RbXe}^{14}$ ) confirm these lifetime estimates. Formation of molecular beams of van der Waals molecules which reduces collisions of course lengthens these lifetimes.

Concentrations of van der Waals molecules have been determined in mass spectroscopy experiments<sup>15</sup> and agree reasonably well with calculations based on an estimation of the number and spacings of bound states.<sup>11</sup> Under favorable experimental conditions, the vapor above the liquid at its boiling point, the concentrations are usually a few percent or less. This explains, in part, why experimental results on van der Waals molecules have been slow to materialize.

Bond lengths in van der Waals molecules can, in principle, be accurately estimated from analysis of rotational fine structure of their spectra. This fine structure is difficult to resolve, however, and only in the case of  $\text{Ne}_2$  has the analysis been possible.<sup>5</sup> The average bond length for  $\text{Ne}_2$  is  $R_0 = 3.1 \text{ \AA}$ . This is the expectation value,  $R_0 = \langle R^{-2} \rangle^{-1/2}$ , for the dimer in its ground vibrational state and is somewhat longer than  $R_e = 2.9 \text{ \AA}$  measured at the bottom of an empirically determined potential curve. The average bond lengths of other van der Waals molecules are shown in Figure 3 as estimated from the MSV functions fit to both spectroscopic and scattering data.<sup>6</sup> These bonds are typically 3–4 Å and are, of course, considerably longer than chemical bonds.

### Polyatomic van der Waals Molecules

van der Waals molecules containing chemically bonded molecules such as  $\text{H}_2\text{-Ar}$ ,  $(\text{O}_2)_2$ , and  $(\text{H}_2\text{O})_2$  are held together by intermolecular interactions which depend on distance and orientation. Since the intermolecular forces used to bind diatomic van der Waals molecules depend only on the distance between two atoms, it is understandable that polyatomic van der Waals molecules are more difficult to describe.

(13) K. Laidler, "Chemical Kinetics", McGraw-Hill, New York, N.Y., 1965.

(14) M. Bouchiat and L. Pottier, *J. Phys. (Paris)*, 33, 213 (1972).

(15) R. E. Leckenby and E. J. Robbins, *Proc. Roy. Soc. London, Ser. A*, 291, 389 (1966).

The molecule  $\text{H}_2\text{-Ar}$  has been extensively studied and is among the best understood of any polyatomic van der Waals molecule. A gaseous mixture of  $\text{H}_2$  and Ar at low temperatures contains a trace of the  $\text{H}_2\text{-Ar}$  van der Waals molecule (as well as  $\text{Ar}_2$  and an exceedingly small amount of  $(\text{H}_2)_2$ ) and its infrared spectrum can be studied at long optical path lengths. (The vibrational spectrum of  $\text{H}_2$  is made weakly infrared active by its bonding to Ar.) A portion of this spectrum reported by McKellar and Welsh<sup>16</sup> is shown in Figure 4. Absorption features occur in regions of the  $Q_1(J)$ ,  $S_1(0)$ , and  $S_1(1)$  electric quadrupole vibration-rotation transitions of free  $\text{H}_2$ . This suggests free (or nearly free) rotational motion of  $\text{H}_2$  within  $\text{H}_2\text{-Ar}$ . The fine structure in each of these regions is associated with end-over-end rotation of the  $\text{H}_2\text{-Ar}$  molecule.

The rotatory motions of a van der Waals molecule of the type  $\text{X}_2\text{-Y}$  (e.g.,  $\text{H}_2\text{-Ar}$ ) are shown in Figure 5. Rotation of  $\text{H}_2$  about its center of mass is given by the  $J$  quantum number and end-over-end rotation of  $\text{H}_2\text{-Ar}$  is given by  $L$ . The quantum number describing the total rotational motion is  $j = J + L, J + L - 1, \dots, |J - L|$ . For absorption with  $J = 0$ , such as  $Q_1(0)$ , the observed fine structure is due to end-over-end rotation alone, yielding a P and R branch. The spacings of these features, due to  $\Delta j = \Delta L = \pm 1$  transitions, were used to determine the average van der Waals bond length of  $R_0 = 3.94 \text{ \AA}$ .

If  $\text{H}_2$  were to rotate freely within  $\text{H}_2\text{-Ar}$  with  $J = 1$  and higher, the spacing of the rotational levels would be like those shown on the left of Figure 6. However, the two types of rotational motions are weakly coupled by the angular dependence of the intermolecular potential, and internal rotation becomes slightly hindered. The barrier to internal rotation is small compared with the spacing of the  $J$  states, so only the  $j$  levels within each  $J$  manifold are significantly shifted. The qualitative appearance of these splittings for *weak coupling* appropriate to  $\text{H}_2\text{-Ar}$  is shown in Figure 6. Experimental evidence for these splittings are the doublets near  $4725 \text{ cm}^{-1}$  in Figure 4. An intermolecular potential function which can

(16) A. R. W. McKellar and H. L. Welsh, *J. Chem. Phys.*, 55, 595 (1971).

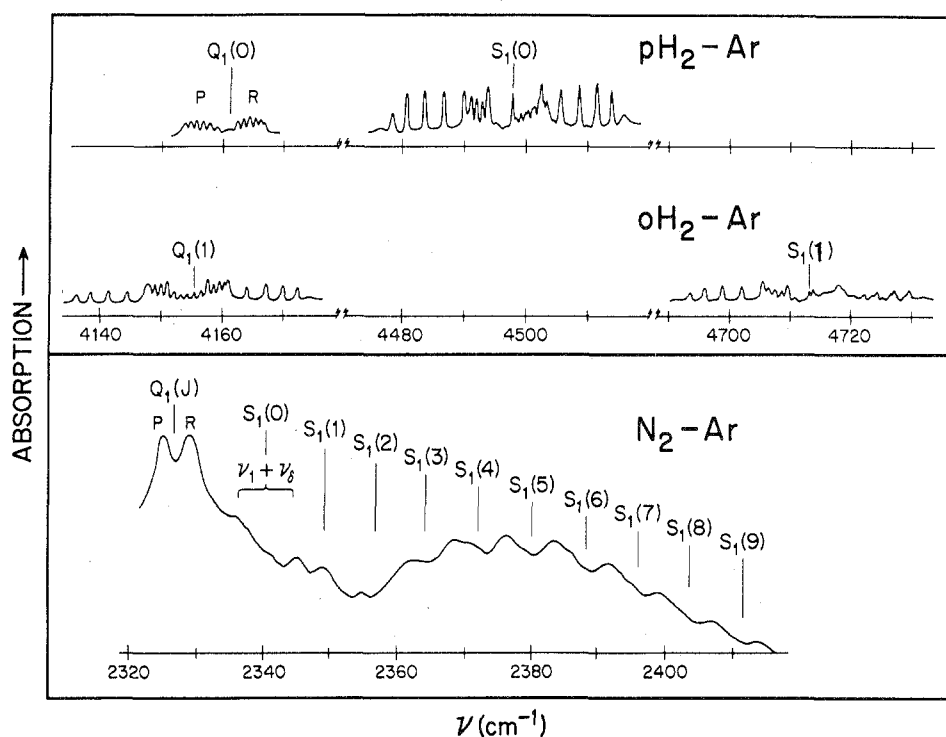


**Figure 4.** Infrared spectrum of  $\text{H}_2\text{-Ar}$  and  $\text{N}_2\text{-Ar}$ .  $\text{H}_2\text{-Ar}$  in an ortho- or para-hydrogen and argon gaseous mixture at pressures of near 0.5 atm and 86 K with an absorption path length of 165 m (A. R. W. McKellar and H. L. Welsh, *J. Chem. Phys.*, **55**, 595 (1971)).  $\text{N}_2\text{-Ar}$  in nitrogen and argon at a pressure near 1 atm at 87 K with an absorption path length of 122 m (G. Henderson and G. E. Ewing, *Mol. Phys.*, **27**, 903 (1974)). The  $Q_1(J)$  and  $S_1(J)$  markers indicate vibration-rotation transition frequencies of the free  $\text{H}_2$  or  $\text{N}_2$  molecule. Vibrational transitions involving the bending mode of  $\text{N}_2\text{-Ar}$  are indicated by  $\nu + \nu_\delta$ .

quantitatively account for the features of the  $\text{H}_2\text{-Ar}$  spectra has been discussed by LeRoy and Van Kranendonk<sup>17</sup> and Dunker and Gordon.<sup>18</sup>

The infrared spectrum of  $\text{N}_2\text{-Ar}$  of Henderson and Ewing<sup>19</sup> is also shown in Figure 4. The vibration-rotation features are more densely spaced than those of  $\text{H}_2\text{-Ar}$  because  $\text{N}_2$  has a larger moment of inertia than  $\text{H}_2$ . Moreover, the features are shifted significantly from the vibration-rotation frequencies of freely rotating  $\text{N}_2$ , in contrast to the near match in the case of  $\text{H}_2\text{-Ar}$ . Finally the  $\text{N}_2\text{-Ar}$  features are diffuse.

For  $\text{N}_2\text{-Ar}$ , in contrast to  $\text{H}_2\text{-Ar}$ , the barrier to internal rotation is large compared with the spacings of the lower  $J$  levels. As a simple model the intermolecular potential for  $\text{N}_2\text{-Ar}$  may be represented by

$$V(R, \theta) = D_e \left[ \left( \frac{R_e}{R} \right)^{12} - 2 \left( \frac{R_e}{R} \right)^6 \right] + \frac{V_0}{2} [\cos 2\theta] \quad (2)$$

The first term in eq 2 is the simple Lennard-Jones 6-12 potential. By ignoring the end-over-end rotation of  $\text{N}_2\text{-Ar}$  the second term in eq 2 can be used to calculate the splitting of the  $J$  states as a function of the barrier to internal rotation,  $V_0$ . (The problem bears some similarity to Stark splitting). The value of  $V_0$  which explains the observed infrared spectrum in Figure 4 is  $V_0 = 0.24$  kJ/mol ( $20 \text{ cm}^{-1}$ ) with a "T" equilibrium configuration. The alternative linear configuration does not fit the data satisfactorily.

For the first few internal rotatory levels, the  $\text{N}_2$  molecule is confined by the potential barrier and undergoes bending vibrations with quantum number  $\nu_\delta$ . The combination of this vibration with the  $\text{N}_2$

(17) R. J. LeRoy and J. Van Kranendonk, *J. Chem. Phys.*, **61**, 4750 (1974).

(18) A. M. Dunker and R. G. Gordon, to be published.

(19) G. Henderson and G. E. Ewing, *Mol. Phys.*, **27**, 903 (1974).

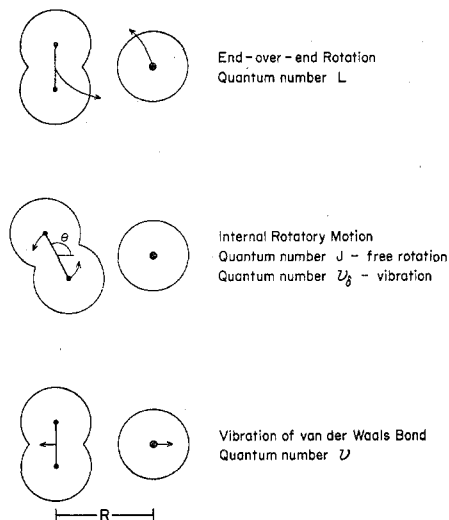


**Figure 5.** Energy modes of an  $\text{X}_2\text{-Y}$  van der Waals molecule. Not shown is the  $\nu_1$  vibrational mode of the  $\text{X}_2$  molecule against its chemical bond.

vibration ( $\nu_1$ ) is labeled  $\nu_1 + \nu_\delta$  in Figure 4.

Higher levels are best described as hindered rotation of  $\text{N}_2$  within  $\text{N}_2\text{-Ar}$ , and this accounts for the mismatch of the multitude of features in Figure 4 with the free rotor  $S_1(J)$  frequencies. At the temperature of experiment, 87 K, roughly 20% of the  $\text{N}_2\text{-Ar}$  molecules are locked into the semirigid "T" structure with large amplitude bending vibrations, and the remaining 80% undergo hindered internal rotation. This structure can be contrasted to that of  $\text{H}_2\text{-Ar}$  where all the molecules are undergoing nearly free internal rotation.

The bond length of  $\text{N}_2\text{-Ar}$  can be estimated from its spectrum.<sup>19</sup> For  $\text{H}_2\text{-Ar}$ , individual  $\Delta L = \pm 1$  tran-

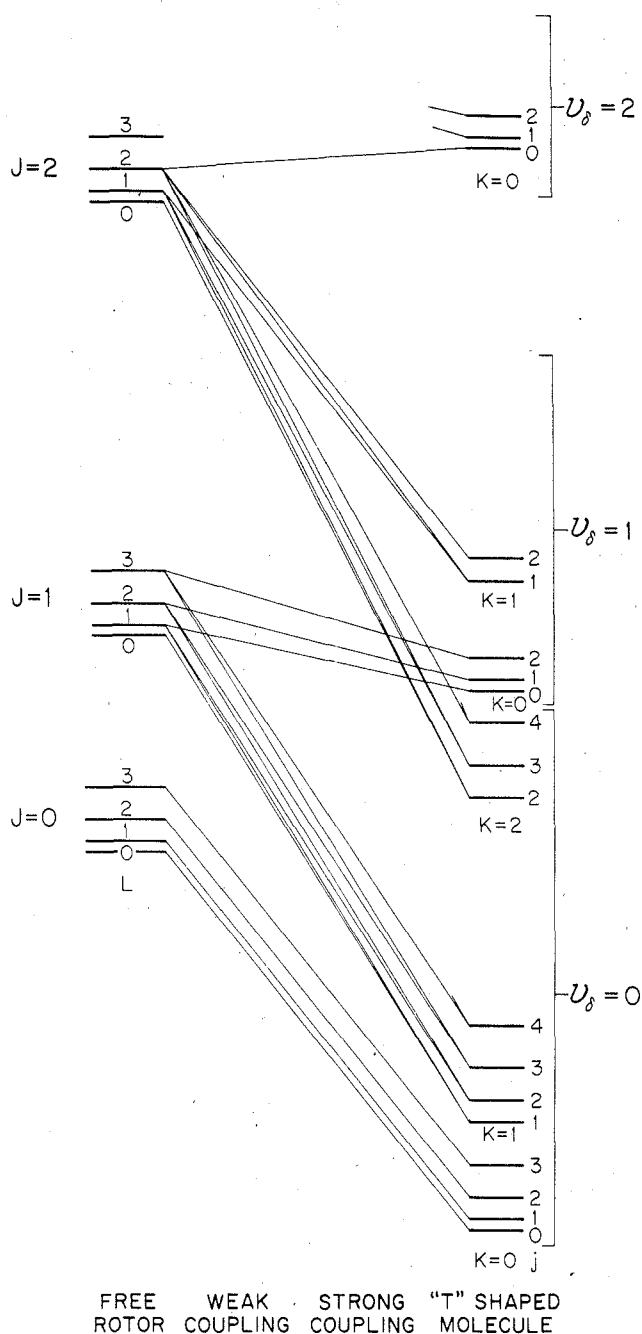


Figure 6. Correlation diagram of rotatory motions of  $X_2$ -Y van der Waals molecules (G. Henderson and G. Ewing, *Mol. Phys.*, 27, 903 (1974)). (Notice that the spacing of the  $L$  levels is much finer than that of the  $J$  levels. This is because  $L$  indicates rotation about the long  $X_2$ -Y van der Waals bond while  $J$  denotes rotation about the short  $X_2$  chemical bond.)

sitions for the single  $J = 0$  state in the lowest  $v = 0$  level could be resolved, and  $R_0$  was determined with considerable precision. For  $N_2$ -Ar, in the Q branch region, closely spaced transitions overlap, and the P and R branches appear as an envelope. A calculated rotational envelope which matches the observed one is consistent with a van der Waals bond length of  $R_0 \approx R_e = 3.9 \pm 0.2 \text{ \AA}$ .

Having evaluated  $R_e$  and  $V_0$  for  $N_2$ -Ar and taking  $D_e = 0.93 \text{ kJ/mol}$  ( $78 \text{ cm}^{-1}$ ) (from nonspectroscopic data<sup>19</sup>), a mapping of eq 2 is possible. This intermolecular potential map is shown in Figure 7. The well depth is modulated by 25% depending on the orientation of  $N_2$  within  $N_2$ -Ar. The minima correspond to the equilibrium "T" configuration. The linear con-

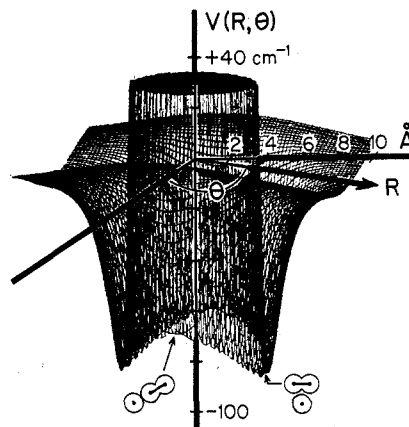


Figure 7. A mapping of the  $N_2$ -Ar intermolecular potential function. A presentation of eq 2 with  $D_e = 0.93 \text{ kJ/mol}$  ( $78 \text{ cm}^{-1}$ ),  $R_e = 3.9 \text{ \AA}$ , and  $V_0 = 0.24 \text{ kJ/mol}$  ( $20 \text{ cm}^{-1}$ ). Positions of the unstable linear configuration ( $\theta = 0^\circ$ ) and the equilibrium, stable, "T" configuration ( $\theta = 90^\circ$ ) are shown. The coordinate system is that given in Figure 5.

figuration is seen to be less stable. This three-dimensional mapping might be compared to the two-dimensional intermolecular potential map for a diatomic van der Waals molecule in Figure 1 or 2.

A more complete theoretical model for  $X_2$ -Y van der Waals molecules would include coupling among internal rotation, end-over-end rotation, and vibration of the van der Waals bond. It is estimated<sup>19</sup> that  $N_2$ -Ar has 10,000 bound states, so this sort of theoretical procedure would be exceedingly involved. For the lighter  $H_2$ -Ar molecule with *weak coupling* and fewer bound states this procedure has been useful.<sup>17,18</sup> In the limit of  $V_0 \rightarrow \infty$  for the T-shaped  $X_2$ -Y molecule all internal rotatory motion appears as  $v_\delta$  bending vibrations. Some of these levels are given to the far right of Figure 6 where  $X_2$ -Y becomes a near-symmetric top. The  $N_2$ -Ar molecule resides somewhere in the *strong coupling* region.

The most precise structural information on van der Waals molecules comes from molecular beam spectroscopy. In an example of these experiments by Novick, Davies, Harris, and Klemperer,<sup>20</sup> a gaseous mixture of HCl and Ar is forced through an expansion nozzle to form a supersonic molecular beam which then contains a small concentration of Ar-HCl. Resonance techniques were used to study microwave ( $\Delta j = 1$ ) and radiofrequency ( $\Delta j = 0$ ,  $|\Delta M_j| = 1$ ) transitions of  $^{40}\text{Ar}$ - $\text{H}^{35}\text{Cl}$  and other isotopes.

As in most structural studies, what is actually determined is an *average* geometry. In this work one structural parameter which is measured is  $\langle \cos \theta \rangle$ , and it corresponds to an angle of  $47.5^\circ$  between the HCl bond and the axis connecting the center of mass of HCl with the Ar. Studies on other isotopes indicate that the *equilibrium* geometry is very nearly linear.<sup>21</sup> The large discrepancy between  $\theta_e \approx 0$  and  $\theta = 47.5^\circ$  from  $\langle \cos \theta \rangle$  is due to the large amplitude motions of hydrogen in the bending vibration. This is a reflection of the semirigid nature of van der Waals molecules as we have just seen in  $N_2$ -Ar.

Only the lowest vibrational state was observed,

(20) S. E. Novick, P. Davies, S. J. Harris, and W. Klemperer, *J. Chem. Phys.*, 59, 2273 (1973).

(21) S. J. Harris, S. E. Novick, and W. Klemperer, *J. Chem. Phys.*, 60, 3208 (1974).

and the average Ar-Cl distance in Ar-HCl was measured to be  $R_0 = 4.006$  Å. Because the H atom makes such large amplitude motions away from the Ar-Cl axis, it is somewhat ineffective in blocking these heavy atoms, and they can approach more closely. The heavier D has smaller amplitude bending motions and the average distance in Ar-DCl is larger,  $R_0 = 4.025$  Å. It was the comparison of these two isotopic molecule bond lengths that indicated that the hydrogen lies between Cl and Ar, giving the structure Ar-HCl and *not* Ar-ClH.

The vibrational frequency of the Ar-HCl van der Waals bond is computed to be  $32.2$   $\text{cm}^{-1}$  from the observed centrifugal distortion constant. The comparable value for Ar<sub>2</sub>, which is isoelectronic with Ar-HCl, is  $25$   $\text{cm}^{-1}$  (see Figure 2). It is the stronger bonding in Ar-HCl which accounts for its higher vibrational frequency.

Since only a few energy levels of Ar-HCl have been determined, an intermolecular potential mapping from spectroscopic data analogous to Figure 7 for N<sub>2</sub>-Ar is not now available. The semirigid equilibrium geometry of Ar-HCl means of course that the barrier to internal rotation exceeds the spacing of the lowest  $J$  levels, as in the case of N<sub>2</sub>-Ar. Transitions within only the lowest  $\nu = \nu_0 = 0$  vibrational state have been reported. The  $j$  states observed are stacked onto the lowest level of the internal rotator manifold in a manner somewhat analogous to that shown in the lower right of Figure 6.

The structure of Ar-ClF has also been determined by electric resonance molecular beam spectroscopy techniques.<sup>22</sup> This structure is compared with those of H<sub>2</sub>-Ar, N<sub>2</sub>-Ar, and Ar-HCl in Figure 3.

Using a path length of 110 m and temperatures near 17 K, McKellar and Welsh studied the infrared spectrum of the trace amount of (H<sub>2</sub>)<sub>2</sub> present in gaseous hydrogen.<sup>23</sup> The many features of this spectrum may be explained by assuming that the H<sub>2</sub> molecules can rotate (nearly) freely within (H<sub>2</sub>)<sub>2</sub>. Because of the weak van der Waals bond and the light mass of H<sub>2</sub>, the  $L = 0$  state of (H<sub>2</sub>)<sub>2</sub> contains only one bound vibrational level,  $\nu = 0$ . The well depth is  $D_e = 0.3$  kJ/mol and the dissociation energy (the energy of the  $L = 0$  level below the dissociation limit) is only  $D_0 = 0.03$  kJ/mol.<sup>24</sup> The dissociation energy of this van der Waals molecule is then 14,000 times smaller than the chemically bonded H<sub>2</sub> molecule!

The  $L = 1, \nu = 0$  state is also bound but has a dissociation energy of only 0.01 kJ/mol. The  $L = 2, \nu = 0$  state, however, is metastable and can tunnel through the centrifugal barrier. Indeed, the observed spectrum involving  $L = 2 \leftarrow L = 1$  transitions is broadened because the lifetime of the  $L = 2$  state is shortened by predissociation while  $L = 1 \leftarrow L = 0$  transitions give sharp narrow absorption features. Measurements of  $L = 1 \leftarrow L = 0$  transitions can be used to determine the moment of inertia and consequently the average bond length of (H<sub>2</sub>)<sub>2</sub> was found to be 4.4 Å.<sup>23</sup> Gordon and Cashion<sup>24</sup> have shown that calculated predissociated band shapes are par-

ticularly sensitive to the intermolecular potential function. Spectroscopic work on other hydrogen isotopes,<sup>23</sup> beam scattering studies,<sup>25</sup> and further theory may provide a rather detailed potential function mapping for (H<sub>2</sub>)<sub>2</sub> in the near future.

The existence of (O<sub>2</sub>)<sub>2</sub> was postulated 50 years ago by G. N. Lewis to explain anomalies in the magnetic properties of liquid oxygen.<sup>26</sup> He suggested that the dimer was stabilized by a weak chemical bond formed by the pairing of electrons of the triplet state ( $^3\Sigma_g^-$ ) O<sub>2</sub> molecules. However, despite a large number of condensed-phase experiments, the positive identification of (O<sub>2</sub>)<sub>2</sub> has not been convincing. Recently, however, Long and Ewing recorded the visible and infrared absorption spectra of (O<sub>2</sub>)<sub>2</sub> in the gas phase at long paths and were able to discuss its structure and properties.<sup>27</sup>

The visible spectrum of (O<sub>2</sub>)<sub>2</sub> contains a number of fine structure features somewhat analogous to those observed in Ar<sub>2</sub> (see Figure 1). These features were assigned to transitions between different stretching vibration levels,  $\nu$ , of the O<sub>2</sub> molecules against the O<sub>2</sub>-O<sub>2</sub> bond. The spacing of these levels suggests a dissociation energy for (O<sub>2</sub>)<sub>2</sub> of 0.9 kJ/mol, which may be compared to 0.92 kJ/mol for Ar<sub>2</sub>. The similarity in these energies suggests that the bonding in (O<sub>2</sub>)<sub>2</sub> and Ar<sub>2</sub> is of the same type. Since the dispersion interactions holding argon atoms together are also present in oxygen, there is no need to propose a pairing of the electrons to form some weak "chemical bond" in (O<sub>2</sub>)<sub>2</sub>.

Fine structure in the infrared region of (O<sub>2</sub>)<sub>2</sub> bears similarities to the rotational components of the N<sub>2</sub>-Ar spectrum (see Figure 4). A detailed analysis has not been possible yet since the anisotropic portion of the intermolecular potential function requires three angles to describe the orientational configuration of O<sub>2</sub> within (O<sub>2</sub>)<sub>2</sub>. However the qualitative appearance of the internal rotational features suggests that, like N<sub>2</sub>-Ar, some of the (O<sub>2</sub>)<sub>2</sub> molecules are locked into a semirigid configuration, but most have O<sub>2</sub> molecules undergoing hindered rotation within the dimer.

Infrared features associated with end-over-end rotation of (O<sub>2</sub>)<sub>2</sub> have been analyzed to give an equilibrium distance of  $R_e = 3.5 \pm 0.2$  Å.<sup>28</sup> A variety of geometries might be selected: rectangular, dihedral, linear, or T-shaped. Strong repulsive interactions from the inner oxygen atoms would make the linear or T-shaped configurations unstable with a distance between the center of masses of the O<sub>2</sub> molecules as short as 3.5 Å. Since O<sub>2</sub> is more polarizable along its bond axis than perpendicular to it, attractive or dispersion forces slightly favor the rectangular over the dihedral configuration.<sup>29</sup> Rectangular (O<sub>2</sub>)<sub>2</sub> seems reasonable therefore for the gas-phase van der Waals molecule.

A weak "chemical bond" is apparently responsible for the stability of (NO)<sub>2</sub> which arises from electron pairing between the two ( $^2\Pi$ ) NO molecules. The

(22) S. J. Harris, S. E. Novick, W. Klemperer, and W. Falconer, *J. Chem. Phys.*, **61**, 193 (1974).

(23) A. R. W. McKellar and H. L. Welsh, *Can. J. Phys.*, **52**, 1082 (1974).

(24) R. G. Gordon and J. K. Cashion, *J. Chem. Phys.*, **44**, 1190 (1966).

(25) J. Farrar and Y. T. Lee, *J. Chem. Phys.*, **57**, 5492 (1972).

(26) G. N. Lewis, *J. Am. Chem. Soc.*, **46**, 2031 (1924).

(27) C. A. Long and G. E. Ewing, *J. Chem. Phys.*, **58**, 4824 (1973).

(28) Calculated from data of ref 27 using the procedure of G. Henderson and G. E. Ewing, *J. Chem. Phys.*, **59**, 2280 (1973).

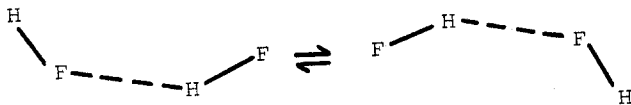
(29) C. A. Long, Ph.D. Thesis, Indiana University, Bloomington, Ind., 1971.

dissociation energy as determined from its electronic spectrum<sup>30</sup> is 6.7 kJ/mol and is considerably greater than that of  $(O_2)_2$ . Its gas-phase infrared spectrum is only observed at low temperatures (120 K) but at a relatively short path length of 5 cm.<sup>31</sup> The bonding in  $(NO)_2$  locks it into a near rectangular cis configuration. The angularly dependent intermolecular forces are so large that bending vibrations rather than hindered rotation dominate the internal rotatory motion of the molecule at 120 K.

The infrared spectrum of carbon dioxide gas reveals a vibration-rotation envelope consistent with T-shaped  $(CO_2)_2$ .<sup>32</sup> The dimer is locked into this orientation by the large molecular quadrupole moment of  $CO_2$ . A similar structure for  $(N_2)_2$  is consistent with its infrared spectrum.<sup>33</sup> However, the small  $N_2$  molecular quadrupole moment allows most of the molecules at 77 K to be undergoing hindered rotation within  $(N_2)_2$ .

Molecular beam electric resonance spectroscopy of the several isotopes of  $(HF)_2$  by Dyke, Howard, and Klemperer<sup>34</sup> has allowed its structure to be determined. This molecule is of particular interest since it represents one of the simplest hydrogen-bonding systems. Because of the hydrogen bond the binding energy ( $D_0 \approx 20$  kJ/mol) is considerably higher than in  $(O_2)_2$  or  $(N_2)_2$  but comparable to that in  $(NO)_2$ . The structure for the dimer is bent with a linear hydrogen bond.

The molecule can flip between two equivalent configurations in which the nonbonded and bonded hydrogens exchange roles:<sup>35</sup>



This occurs by quantum mechanical tunneling through a potential barrier and bears a close analogy to the "umbrella" inversion observed in  $NH_3$ . The tunneling in both cases proceeds at a rate that leads to observable doubling of the rotational energy levels. The barrier height for the tunneling in  $(HF)_2$  is about 6 kJ/mol. A complete mapping of the intermolecular potential as a function of the three orientational angles and dimer bond length must await further spectroscopic and theoretical work.

A preliminary report on the structure of the water dimer has been given by Dyke and Muentner;<sup>36</sup> like  $(HF)_2$ , it also contains a linear hydrogen bond. Since  $(H_2O)_2$  is defined by the dimer bond distance and seven internal angles, its structure is the most complex so far discussed. Because any one of the four protons can form the hydrogen bond, a number of equivalent configurations are possible for  $(H_2O)_2$  and tunneling between these configurations leads to observable splittings of the rotational states. This com-

plication, while containing useful information on the intermolecular potential of the dimer, has made analysis of its molecular beam electric resonance spectrum exceedingly difficult. Because of the great importance of understanding hydrogen bonding in water, further analysis of the spectroscopic data for determining the properties of the dimer will be particularly interesting.

### van der Waals Molecules: Some Comparisons

The structures of the van der Waals molecules discussed here can be compared in Figure 3. The bond lengths are presented according to  $R_0$  values, and the bond angles represent the equilibrium configurations. The spheres around each atom have radii equal to their van der Waals radii. For the rare gas atoms the radii are calculated from nearest-neighbor distances in the crystal.<sup>37</sup> The radii around other atoms conform to Pauling's frequently used estimates.<sup>38</sup>

The observed rare gas dimer bond lengths agree closely with the sum of the van der Waals radii drawn. This says that the crystal bond lengths for the many-body solid-state system very nearly equal van der Waals molecule bond lengths for dimers in the gas phase. The close agreement between the bond lengths tends to support the usual approximation that intermolecular energies are pairwise additive in the condensed state. However, part of the agreement is due to cancellations of non-nearest-neighbor attractive interactions, three-body interactions, and the effects of zero-point vibrations in the solid.<sup>39</sup>

The van der Waals radii and gas-phase structures are not so consistent for the other molecules listed in Figure 3 for a variety of reasons. In the cases of  $(HF)_2$ ,  $(H_2O)_2$ , and  $(NO)_2$  the van der Waals radii overlap considerably. For these molecules, however, the dissociation energy is an order of magnitude greater than that for the rare gas dimers. The hydrogen bonding in  $(HF)_2$  and  $(H_2O)_2$  and the pairing of the odd electrons to form  $(NO)_2$  can account for the stronger bonding and shorter intermolecular distances in these molecules. The geometries assumed by  $(HF)_2$  and  $(H_2O)_2$  (which are isoelectronic) are determined by hydrogen bonding to lone-pair electrons on the acceptor atom. Following the simple picture of lone-pair spacial arrangements the resulting near-tetrahedral bond angles found in both  $(HF)_2$  and  $(H_2O)_2$  seem reasonable. Bonding in  $(NO)_2$  is believed to involve an overlap of p orbitals between both nitrogen and oxygen atoms to form weak  $\sigma_{N-N}$  and  $\sigma_{O-O}$  bonds which lock the molecule into a cis configuration.<sup>40</sup>

In the molecules  $Ar-HCl$ ,  $Ar-ClF$ , and  $(CO_2)_2$  there is a slight overlap of van der Waals radii that suggests bonding forces in addition to dispersion. Linear  $Ar-HCl$  with hydrogen between the larger atoms may indicate a weak hydrogen bond. It has been suggested<sup>22</sup> that Walsh-type rules<sup>41</sup> originally

(30) J. Billingsley and A. Callear, *Trans. Faraday Soc.*, **67**, 589 (1971).

(31) C. E. Dinerman and G. E. Ewing, *J. Chem. Phys.*, **53**, 626 (1970); **54**, 3660 (1971).

(32) L. Mannik, J. C. Stryland, and H. L. Welsh, *Can. J. Phys.*, **49**, 3056 (1971).

(33) C. A. Long, G. Henderson, and G. E. Ewing, *Chem. Phys.*, **2**, 465 (1973).

(34) T. Dyke, B. J. Howard, and W. Klemperer, *J. Chem. Phys.*, **56**, 2442 (1972).

(35) W. Klemperer, *Ber.*, **78**, 128 (1974).

(36) T. Dyke and J. Muentner, *J. Chem. Phys.*, **60**, 2929 (1974).

(37) R. W. G. Wyckoff, "Crystal Structures", 2nd ed., Vol. 1, Interscience, New York, N.Y., 1960.

(38) L. Pauling, "The Nature of the Chemical Bond", 3rd ed, Cornell University Press, Ithaca, N.Y., 1960.

(39) See ref 8b.

(40) C. Bibart and G. Ewing, *J. Chem. Phys.*, **61**, 1284 (1974). See also P. Skancke and J. Boggs, *Chem. Phys. Lett.*, **21**, 316 (1973).

developed for predicting structures of chemically bonded molecules can be useful for discussing complexes like ArClF. Applying the Walsh rules for triatomic molecules, ArClF is predicted to be linear, with Cl the central atom, as is observed. The molecular quadrupole moment of CO<sub>2</sub> is large. The difference in electrostatic quadrupole-quadrupole interaction in (CO<sub>2</sub>)<sub>2</sub> at 4.1 Å between linear (repulsive) and T (attractive) configurations is 8 kJ/mol.<sup>42</sup> It is not surprising, then, that the equilibrium structure is T-shaped, with a relatively short intermolecular bond.

For H<sub>2</sub>-Ar and (H<sub>2</sub>)<sub>2</sub> the intermolecular bond is significantly greater than the sum of van der Waals radii. For these hydrogen-containing molecules this discrepancy may reside in the way the structures have been represented. The values of bond length  $R_0$  are much longer than, e.g.,  $R_e$  (for (H<sub>2</sub>)<sub>2</sub>  $R_e \sim 3.0$  Å,  $R_0 \sim 4.4$  Å) because of the unusually large amplitude vibration of the light H<sub>2</sub> molecule against the weak intermolecular bond. Had a value nearer  $R_e$  been presented in Figure 3, the van der Waals structures would have been more consistent with the van der Waals radii. These near-free-rotor structures are represented by the arrows in Figure 3.

The discrepancy between intermolecular bond lengths and van der Waals radii for the remaining molecules N<sub>2</sub>-Ar, (N<sub>2</sub>)<sub>2</sub>, and (O<sub>2</sub>)<sub>2</sub> may be due in part to errors in determining the bond lengths. The structures can be rationalized by discussing the delicate balance among anisotropic dispersion, quadrupole, and repulsive forces. In the case of (O<sub>2</sub>)<sub>2</sub>, as discussed earlier, the anisotropic dispersion forces stabilize the rectangular geometry. For (N<sub>2</sub>)<sub>2</sub>, quadrupole-quadrupole interactions favor the T configuration as in the case of (CO<sub>2</sub>)<sub>2</sub>. (The quadrupole mo-

ment of N<sub>2</sub> is smaller than that of CO<sub>2</sub> but larger than O<sub>2</sub>.) It has been argued<sup>19</sup> that the T configuration of N<sub>2</sub>-Ar, rather than the linear arrangement, is favored because repulsive interactions are minimized while dispersion interactions operate effectively.

In all cases where crystal structure can be compared to the polyatomic van der Waals molecule structure the general molecular arrangements are in agreement. Evidence for the zig-zag hydrogen bond is found in ice<sup>43</sup> and solid HF.<sup>44</sup> Rectangular or near-rectangular structures are reported for solid nitric oxide<sup>45</sup> and oxygen.<sup>46</sup> A near-T configuration is found in solid nitrogen<sup>47</sup> and carbon dioxide.<sup>48</sup> Evidence for nearly free rotation is found in solid hydrogen.<sup>49</sup> However, in many of these cases significant discrepancies exist for the bond lengths.

### Summary

Studies of van der Waals molecules provide a new source of information to map intermolecular interactions, augmenting that available from molecular beam scattering and macroscopic measurements. It is apparent that arguments used to discuss bonding in most van der Waals molecules are made with more confidence when the structures and properties are known beforehand. With the present excitement and interest in van der Waals molecules, it may not be long before our knowledge of intermolecular interactions will allow a more substantial understanding of this new class of molecules.

*This work was supported by the National Science Foundation under Grant GP-37043X1.*

(43) For example, see discussion in ref 38, p 464 ff.

(44) M. Atoji and W. N. Lipscomb, *Acta Crystallogr.*, **7**, 173 (1954).

(45) W. Lipscomb, F. Wang, W. May, and E. Lippert, Jr., *Acta Crystallogr.*, **14**, 1100 (1961).

(46) C. Barrett, L. Meyer, and J. Wasserman, *J. Chem. Phys.*, **47**, 592 (1967).

(47) T. Jordon, H. Smith, W. Streib, and W. Lipscomb, *J. Chem. Phys.*, **41**, 756 (1964).

(48) W. Keesom and J. Köhler, *Physica*, **1**, 167, 655 (1934).

(49) J. van Kranendonk and H. P. Gush, *Phys. Lett.*, **1**, 22 (1962).

(41) A. D. Walsh, *J. Chem. Soc.*, 2266 (1953).

(42) Using the coupling constant  $3\theta/4R_0^5 = 0.7$  kJ/mol from ref 32 and orientational factors from A. Buckingham, *Q. Rev., Chem. Soc.*, **13**, 183 (1959).

## Some Progeny of 2,3-Unsaturated Sugars—They Little Resemble Grandfather Glucose

Bert Fraser-Reid

*Department of Chemistry, University of Waterloo, Waterloo, Ontario Canada*

*Received July 16, 1974*

The author has been both praised and abused for using carbohydrate derivatives "to do organic chem-

Bert Fraser-Reid was born in Jamaica, received his primary and secondary education there, and then worked for 5 years during which time he made his first acquaintance with chemistry. He emigrated to Canada and obtained his B.Sc. and M.Sc. (with J. K. N. Jones) at Queen's University, Kingston, Ontario, and his Ph.D. in 1964 at the University of Alberta (Edmonton) under R. U. Lemieux. After 2 years of postdoctoral study with Sir Derek Barton at Imperial College, London, he joined the fledgling University at Waterloo in 1966 where he is currently an Associate Professor. He is an accomplished musician on the pipe organ and piano.

istry". One friend allowed that there are aspects of sugar chemistry which deserve the attention of competent chemists, while another expressed amazement that we know how to use a drybox since sugars are water soluble. A Nobel Laureate known to the author declared that the stabilization of the anomeric cation by the ring oxygen constitutes half of sugar chemistry. A graduate student (from another area) was amazed to find that many of the fabled mysteries of the hexoses garnered during that fateful 2 weeks of Org. Chem. II disappeared once he drew the